Local polarization switching in stressed ferroelectric polymers

Ronggang Cai, Bernard Nysten, Zhijun Hu, and Alain M. Jonas

Citation: Appl. Phys. Lett. **110**, 202901 (2017); doi: 10.1063/1.4983609
View online: http://dx.doi.org/10.1063/1.4983609
View Table of Contents: http://aip.scitation.org/toc/apl/110/20
Published by the American Institute of Physics

Local polarization switching in stressed ferroelectric polymers

Ronggang Cai,[1,a)] Bernard Nysten,[1] Zhijun Hu,[2] and Alain M. Jonas[1,a)]
[1]*Bio & Soft Matter, Institute of Condensed Matter and Nanosciences, Université catholique de Louvain, Croix du Sud 1/L7.04.02, 1348 Louvain-la-Neuve, Belgium*
[2]*Center for Soft Condensed Matter Physics and Interdisciplinary Research, Soochow University, 215006 Suzhou, China*

(Received 28 November 2016; accepted 28 April 2017; published online 15 May 2017)

Ferroelectric polymers are used in flexible organic ferroelectric memories, ferroelectric polarization enhanced organic solar cells, and organic multiferroics. Therefore, understanding their polarization switching mechanism under bending is important for the operation of such devices. Here, we study locally by piezoresponse force microscopy (PFM) polarization switching in bent thin films of the ferroelectric polymer poly(vinylidene fluoride-*ran*-trifluoroethylene). In bent samples, higher probability of domain nucleation, faster domain wall propagation, and lower coercive field are consistently observed by PFM. We ascribe these observations to a decrease of the domain wall pinning energy, resulting from the mechanical energy stored in the sample due to bending in the presence of the compression gradient generated below the PFM tip. *Published by AIP Publishing.*
[http://dx.doi.org/10.1063/1.4983609]

Ferroelectric polymers have been extensively studied over the past decades, owing to their interest for the fabrication of flexible organic ferroelectric memories.[1–12] Among ferroelectric polymers, poly(vinylidene fluoride-*ran*-trifluoroethylene) (P(VDF-TrFE)) is especially attractive due to its large remnant polarization, high flexibility, reasonable cost, high chemical and physical stability, and ease of production and processing.[13–15] Importantly, P(VDF-TrFE) also offers a robust and model system for the fundamental studies of organic ferroelectrics.[6,16–21] For instance, ferroelectricity could be demonstrated to exist in ultrathin films prepared by Langmuir-Blodgett deposition of a few P(VDF-TrFE) monolayers only.[6,16]

In flexible memory devices, it is important to understand how the ferroelectric polymer behaves when bent. A few reports have studied the influence of bending on the remnant polarization and coercive field of P(VDF-TrFE) films,[22–26] and a few others investigated the memory performance of ferroelectric memories employing P(VDF-TrFE) in combination with semiconductors.[24,26–31] A slight increase of remnant polarization was sometimes observed upon bending, but no significant shift of coercive field nor variation of transistor characteristics could be observed, excluding fatigue effects, even down to sub-millimeter radii of curvature.[29]

However, so far, no study had investigated the local dynamics of switching of polarized domains in bent P(VDF-TrFE). In unstrained polycrystalline P(VDF-TrFE) thin films, non-thermally activated (cold-field) polarization switching was observed, which implies heterogeneous nucleation of domains in contrast to intrinsic switching. In this case, defects in chain conformations and chain packing of P(VDF-TrFE) play an important role in the polarization switching and spatial domain growth velocity.[17–19] Recently, we showed that polarization switching is also controlled by the hierarchical structure of P(VDF-TrFE) thin films. Due to its semicrystalline nature, P(VDF-TrFE) typically organizes into crystalline lamellae with folded chains separated by amorphous regions consisting of sharp folds, loose loops, tie segments, and dangling ends of the polymer chains. Based on this structure, we proposed a two-step polarization switching mechanism consisting of domain wall flow motion within P(VDF-TrFE) lamellae with pinning arising from the presence of amorphous regions. The propagation of the switched domain boundary requires an external activation energy to overcome the pinning energy, resulting in creep-like motion from lamella to lamella.[20] When bent, strains will distribute heterogeneously between crystalline and softer amorphous regions, which should change the overall dynamics of domain wall motion, an hypothesis which will be tested here.

In this work, we thus systematically study by piezoresponse force microscopy (PFM) local polarization switching in bent P(VDF-TrFE) thin films. To prepare the test samples, *ca.* 100 nm thick P(VDF-TrFE) (65/35 weight %) films were spincoated from a solution on a polyimide sheet (thickness $d = 260\ \mu$m) coated by 5/50 nm Cr/Au [Fig. 1(a)]. The samples were then annealed at 135 °C for 10 min. A Pt/Ir coated conductive tip of nominal radius $a = 20$ nm (SCM-PIT from

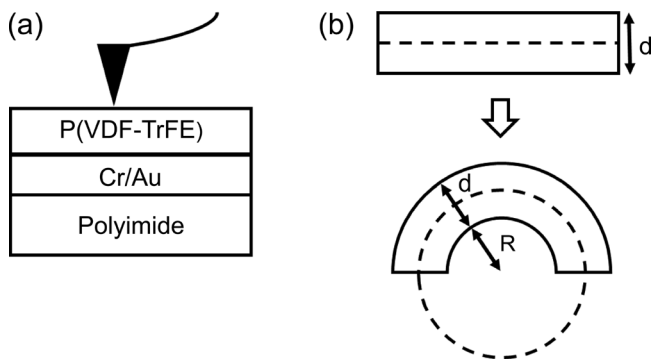

FIG. 1. (a) Sample structure with PFM tip as top electrode. (b) Schematic drawings of the flat and bent sample (bending radius R). P(VDF-TrFE) and Cr/Au electrode layers are not represented because the total thickness of these layers is much smaller than the thickness d of the polyimide substrate.

[a)]Authors to whom correspondence should be addressed: ronggang.cai@uclouvain.be and alain.jonas@uclouvain.be

Bruker) was used to pole the sample and monitor the polarization switching of P(VDF-TrFE). All PFM phase images and hysteresis loops were obtained with a Bruker Icon Dimension by applying an ac voltage of 2 V amplitude and 200 kHz frequency (close to the contact resonance, *ca.* 220 kHz) to the sample while keeping the tip grounded, or sweeping the tip voltage from −10 V to 10 V, and back to −10 V. The force applied to the tip was ∼50 nN, reasonably below the threshold for mechanical force-induced polarization switching.[32]

Mechanical tensile stresses were applied to P(VDF-TrFE) by bending the sample over a solid cylinder of radius R, as shown in Fig. 1(b). Since the total thickness of P(VDF-TrFE) and Cr/Au electrode layers is negligible compared to the thickness d of the substrate, the tensile strain can be calculated as $\varepsilon = \frac{d}{2R+d} \approx \frac{d}{2R}$, and the gradient of strain in the vertical (z) direction is $\frac{\partial \varepsilon}{\partial z} = \frac{2}{2R+d} \approx \frac{1}{R}$, when the bending radius is significantly larger than d. Here, the bending radii R were 47.5 mm, 37.5 mm, 20 mm, 14 mm or 7.5 mm, corresponding to tensile strains of 0.27%, 0.35%, 0.65%, 0.92%, and 1.70%, respectively. No mechanical failure is expected for the Au electrode for tensile strains below 2%.[33]

In such bent films, both piezoelectricity and flexoelectricity may contribute to changing polarization. Piezoelectricity results from a change in atomic distances following the application of a stress; flexoelectricity is due to the asymmetrical shape of the polar elements of a material, which reorient in a strain gradient to minimize deformation energy. The piezoelectric coefficients d_{ij} of P(VDF-TrFE) are well-known and range from *ca.* −40 to 10 pC/N depending on orientation.[34] Therefore, considering a Young's modulus E of *ca.* 2 GPa, the piezoelectric change of polarization in our samples is at most *ca.* 1 mC/m^2 for the smaller bending radius. This variation of polarization remains well below the remanent polarization of P(VDF-TrFE) of *ca.* 70 mC/m^2.[35]

The flexoelectric coefficient μ of P(VDF-TrFE) was reported to be giant in the range of 80 μC/m;[36] however, much more modest values, less than 191 nC/m, were subsequently measured by Poddar and Ducharme,[37,38] compatible with early measurements by Fukada *et al.* (*ca.* 70 nC/m).[39] Therefore, the ratio between the change of polarization due to flexoelectricity and piezoelectricity, $\Delta P_{\text{flexo}}/\Delta P_{\text{piezo}} = (2/d)(\mu/E)\, d_{ij}$, is very small (3%), showing that bending-induced flexoelectricity can be safely ignored in our experiments.

Figures 2(a)–2(c) show PFM phase images (obtained for exactly the same PFM operating conditions) at 0%, 0.27%, and 0.35% tensile strains, respectively. The sample was poled upward over a large region; then short 10 V voltage pulses (0.5 s) were applied locally to switch polarization before PFM imaging. All reversal domains are approximately circular with moderately rough edges, which is in line with the previous observations.[18,19] Noticeably, the domains become larger with increasing strain; the resulting domain size as a function of tensile strain is plotted in Fig. 2(d), suggesting that tensile strains facilitate polarization switching and domain wall propagation. Here, the domain size is defined as the average radius of the roughly circular domain and is calculated as $\sqrt{S/\pi}$, where S is the area of each switched domain in PFM phase images. The easier polarization switching and domain growth indicate that

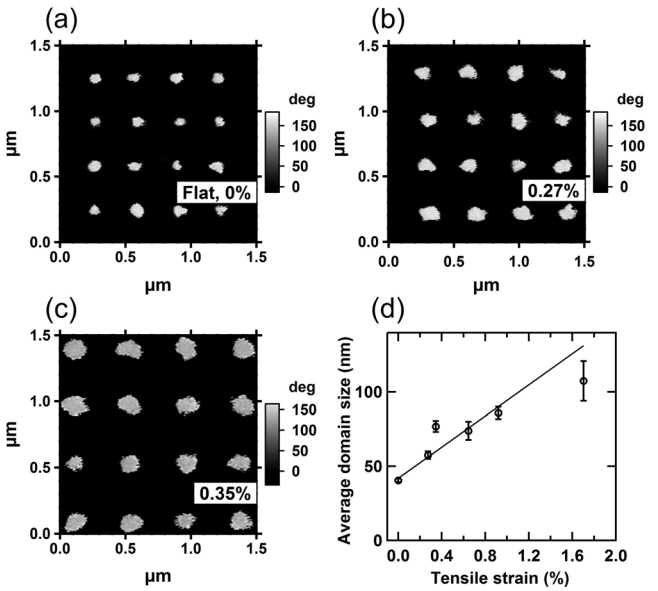

FIG. 2. PFM phase images of a ferroelectric P(VDF-TrFE) film with tensile strains of (a) 0% (flat film), (b) 0.27%, and (c) 0.35%. In all images, the large background regions (black) were first poled by applying a −10 V dc voltage on the tip, while keeping the bottom electrode grounded. The reversal domains (white, 16 in each image) were generated by fixing the tip at approximately the center of each domain while applying a voltage pulse of 10 V for 0.5 s. The average domain size as a function of the tensile strain is plotted in (d).

the added mechanical strain energy contributes to lower the activation energy for domain nucleation and/or domain wall propagation (depinning), resulting in larger domain sizes.

PFM phase images in Figs. 3(a) and 3(b) show the domains switched by applying voltage pulses of different amplitudes for a same duration of 1 s, in the case of 0% and 0.35% tensile strains. The average domain size tends to be larger for the same voltage pulse amplitude in the strained film compared to the flat one, which is consistent with the observation in Fig. 2. We statistically define the probability of domain nucleation as $\frac{N_{switch}}{N_{total}}$, where N_{switch} is the number of nucleated domains and N_{total} is the number of total domains at which a certain poling voltage is applied. A domain is considered as nucleated as soon as a white pixel appears at the proper location in the PFM images. The probability of domain nucleation is plotted in Fig. 3(c) versus the amplitude of the voltage pulses. The critical electric field for domain nucleation (defined as the electric field at half maximum of the switching probability) can be extracted from Fig. 3(c); it is *ca.* 63 MV/m and 54 MV/m in the presence of 0% and 0.35% strain, respectively. For the flat sample, this critical field is reasonably close to the coercive field of bulk P(VDF-TrFE), 61.5 MV/m measured on the same polymer grade by another methodology.[10] The smaller critical field of the stressed sample indicates easier nucleation of the polarization reversal.

PFM phase images in Figs. 4(a) and 4(b) show the domains switched by applying voltage pulses of different durations with a same amplitude of 10 V, for 0% and 0.35% tensile strains. The domain size is in general larger for the same voltage pulse duration in the stressed film compared to the flat one, which is again consistent with our previous observations. In agreement with the previous reports,[20,40] the average domain size grows logarithmically with pulse duration, when

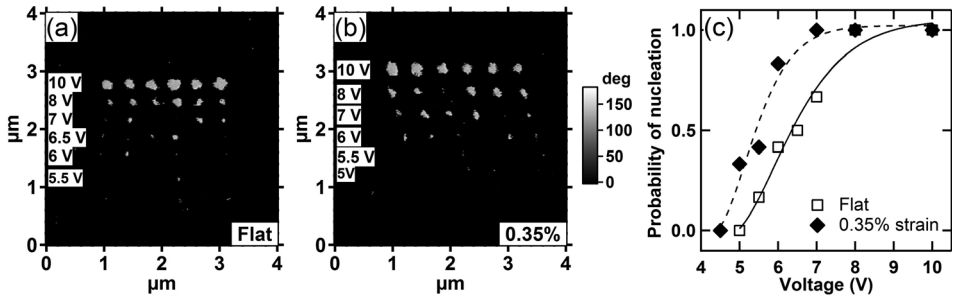

FIG. 3. PFM phase images of a P(VDF-TrFE) film with tensile strains of (a) 0% (flat film) and (b) 0.35%. The scale bar for both images is shown at the right side of (b). The background (black) was first poled by applying a −10 V dc voltage on the tip, while keeping the bottom electrode grounded. The reversal domains (white) were generated by fixing the tip at approximately the center of each domain with different voltage pulses (indicated in each image, 1 s duration) dedicated to each row. (d) The probability of domain nucleation (calculated based on 12 attempts for each voltage) is plotted as a function of the tip poling voltage. The solid and dashed lines are drawn to guide the eye.

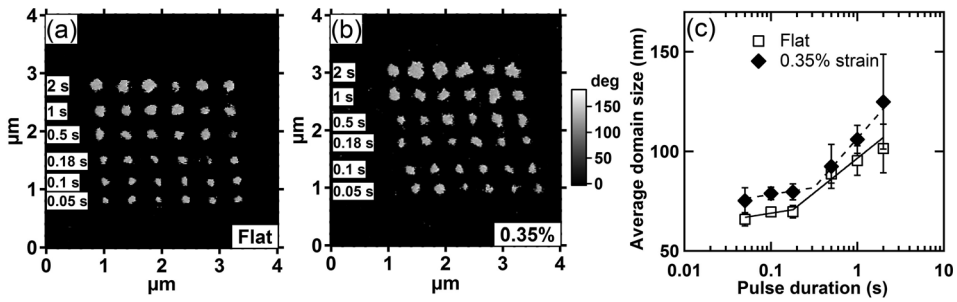

FIG. 4. PFM phase images of a P(VDF-TrFE) film with tensile strains of (a) 0% (flat film) and (b) 0.35%. The scale bar for both images is shown at the right side of (b). In both images, the whole background regions (black) were first poled by applying a −10 V dc voltage on the scanning PFM tip while keeping the sample grounded. The reversal domains (white, 36 domains in each image) were generated by fixing the tip at approximately the center of each domain and applying 10 V voltage pulses with different pulse durations (indicated in each image) dedicated to each row, while keeping the sample grounded. The average domain size as a function of voltage pulse duration is plotted in (c).

the duration is larger than 0.18 s [Fig. 4(c)]. In addition, the rate of domain growth is slightly larger for the stressed film, showing that domain walls propagate slightly faster when the film is bent. Hence, both domain nucleation [Fig. 3(c)] and domain growth [Fig. 4(c)] are favored by the application of a tensile strain. When the duration is smaller than 0.18 s, the domain size becomes almost constant in both cases, *ca.* 68 and 78 nm for the flat and stressed films, respectively. The larger domain size for the stressed film in this small-time scale regime results from its higher probability of domain nucleation. As for the change of slope in the short duration regime, it is discussed later in this article.

To further demonstrate that mechanical stress/strain facilitates global polarization switching, PFM phase hysteresis loops were recorded on the flat and bent films. Figure 5(a) shows typical hysteresis loops for 0%, 0.27%, and 1.70% tensile strain. The loop width decreases with increasing strain, consistent with increased domain nucleation and wall propagation rates. Successive measurements of the PFM hysteresis loops indicate that the first two or three loops have a significantly smaller width than the next ones, for the flat sample and the 0.27% strain sample [Fig. 5(b)]; we ascribe this effect to residual stresses introduced in the film during the installation of the sample onto the PFM setup. These stresses are relaxed by the segmental molecular motions generated during the first probing cycles. When averaged over many successive cycles, excluding the 2 first ones, the average hysteresis loop width decreases with tensile strain [Fig. 5(c)], showing that the coercive field decreases for stressed P(VDF-TrFE), which again is consistent with our previous results.

We have thus demonstrated that the polarization behavior of P(VDF-TrFE), when measured by PFM, is significantly affected by mechanical stresses/strains. In bent samples, higher probability of domain nucleation, faster wall propagation, and lower coercive field are consistently observed by PFM. This is most likely due to a decrease of nucleation and pinning barriers by the mechanical energy stored in the sample, which eases the motion of chain segments during switching. However, it remains to understand why these effects were not detected in previous non-local experiments

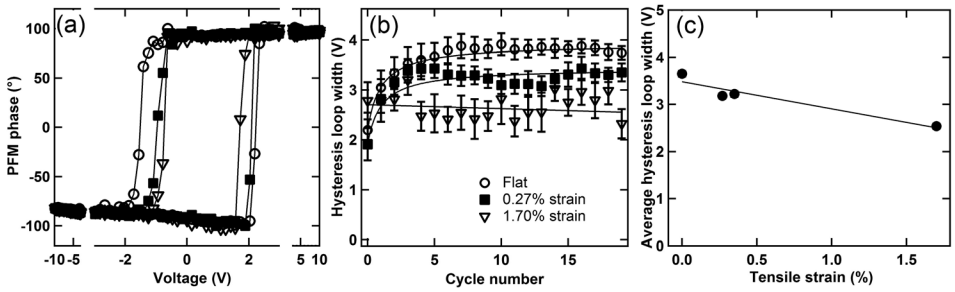

FIG. 5. Typical PFM phase hysteresis loops (a) and loop width as a function of measurement cycle number for samples with 0%, 0.27%, and 1.70% tensile strain. The legend shown in (b) is the same for (a). The average PFM hysteresis loop width is plotted in (c) versus tensile strain. The solid lines in all panels are guide to the eyes.

performed in capacitor or transistor configurations, although the used range of strains are comparable.

A probable cause is the added effect of the force resulting from the PFM tip. It was recently shown that mechanical switching of the electrical polarization can be achieved by the local application of forces with the tip of an atomic force microscopy (AFM), for both inorganic ferroelectric materials[41] and P(VDF-TrFE).[32] This was linked to flexoelectricity and the existence of very large strain gradients below the tip. In our experiments, we used low application forces to minimize this effect; nevertheless, the addition of tip-created strain gradients to the stressed state of the bent sample might still favor a faster nucleation of reversed domains. Contact mechanics indicates that, with a tip radius of 20 nm, a force of 50 nN and a Young's modulus of 2 GPa, a significant compressive strain exists in the sample below the tip, over a range of 20–40 nm. The deformation state of the sample is thus complex in the experiments, and tip-induced nucleation of domain switching might actually be the reason for the change of slope seen in Fig. 4(c) at short pulse durations. However, mechanical effects from the tip alone cannot explain the faster domain growth away from the contact point (Figs. 2 and 4) because strain gradients are essentially limited to the tip contact area and below; nor can they explain the differences consistently seen between the differently bent samples which are probed with similar tip application forces. At this stage, the precise molecular mechanisms explaining the faster polarization switching under a stress are not fully understood. It is however sure that strains concentrate in the softer amorphous interlamellar regions and at crystal/amorphous interfaces; this might result in an increase of the proportion of *trans* vs. *gauche* bonds in these regions that would ease domain wall propagation from crystal to crystal.

In summary, we have shown that when P(VDF-TrFE) films are stretched and probed by PFM, faster domain nucleation and wall propagation are observed for higher stretching ratios. These effects are most probably partially controlled by the additional presence of a strain gradient arising from the PFM probe and illustrate that mechanical forces and their gradients can play an important role for the control of switching, possibly through a change in the proportion of rotational isomers in amorphous regions and at crystal/amorphous interfaces. This might actually explain our recent finding of polarization switching induced by magnetostriction-mediated strains in hybrid magnetic/ferroelectric nanopatterned composite films based on P(VDF-TrFE).[42] At any rate, our results suggest that proper local design of internal stresses may provide a supplementary handle to design ferroelectric devices and to optimize the performance of organic ferroelectric memories and organic multiferroics.

Financial support was provided by the Belgian Science Policy (IAP P6/27), the Wallonia/Brussels Community (ARC 13/18-052), and the Belgian Fund for Scientific Research (FNRS).

[1]R. C. G. Naber, C. Tanase, P. W. M. Blom, G. H. Gelinck, A. W. Marsman, F. J. Touwslager, S. Setayesh, and D. M. de Leeuw, Nat. Mater. **4**(3), 243 (2005).
[2]K. Asadi, D. M. de Leeuw, B. D. Boer, and P. W. M. Blom, Nat. Mater. **7**(7), 547 (2008).
[3]Z. Hu, M. Tian, B. Nysten, and A. M. Jonas, Nat. Mater. **8**(1), 62 (2009).
[4]M. Li, H. J. Wondergem, M.-J. Spijkman, K. Asadi, I. Katsouras, P. W. M. Blom, and D. M. de Leeuw, Nat. Mater. **12**(5), 433 (2013).
[5]I. Katsouras, K. Asadi, M. Li, T. B. van Driel, K. S. Kjaer, D. Zhao, T. Lenz, Y. Gu, P. W. M. Blom, D. Damjanovic, M. M. Nielsen, and D. M. de Leeuw, Nat. Mater. **15**(1), 78 (2016).
[6]A. V. Bune, V. M. Fridkin, S. Ducharme, L. M. Blinov, S. P. Palto, A. V. Sorokin, S. G. Yudin, and A. Zlatkin, Nature **391**(6670), 874 (1998).
[7]H. G. Kassa, R. Cai, A. Marrani, B. Nysten, Z. Hu, and A. M. Jonas, Macromolecules **46**(21), 8569 (2013).
[8]R. Cai, H. G. Kassa, A. Marrani, A. J. J. M. van Breemen, G. H. Gelinck, B. Nysten, Z. Hu, and A. M. Jonas, Appl. Phys. Lett. **105**(11), 113113 (2014).
[9]L. Nougaret, H. G. Kassa, R. Cai, T. Patois, B. Nysten, A. J. J. M. van Breemen, G. H. Gelinck, D. M. de Leeuw, A. Marrani, Z. Hu, and A. M. Jonas, ACS Nano **8**(4), 3498 (2014).
[10]R. Cai and A. M. Jonas, Sci. Rep. **6**, 22116 (2016).
[11]R. Cai, H. G. Kassa, R. Haouari, A. Marrani, Y. H. Geerts, C. Ruzie, A. J. J. M. van Breemen, G. H. Gelinck, B. Nysten, Z. Hu, and A. M. Jonas, Nanoscale **8**(11), 5968 (2016).
[12]S. Horiuchi and Y. Tokura, Nat. Mater. **7**(5), 357 (2008).
[13]T. Furukawa, Phase Transitions **18**(3–4), 143 (1989).
[14]Q.-D. Ling, D.-J. Liaw, C. Zhu, D. S.-H. Chan, E.-T. Kang, and K.-G. Neoh, Prog. Polym. Sci. **33**(10), 917 (2008).
[15]S. Ducharme and A. Gruverman, Nat. Mater. **8**(1), 9 (2009).
[16]S. Ducharme, V. M. Fridkin, A. V. Bune, S. P. Palto, L. M. Blinov, N. N. Petukhova, and S. G. Yudin, Phys. Rev. Lett. **84**(1), 175 (2000).
[17]I. Stolichnov, P. Maksymovych, E. Mikheev, S. V. Kalinin, A. K. Tagantsev, and N. Setter, Phys. Rev. Lett. **108**(2), 027603 (2012).
[18]P. Sharma, T. J. Reece, S. Ducharme, and A. Gruverman, Nano Lett. **11**(5), 1970 (2011).
[19]Z. Xiao, S. Poddar, S. Ducharme, and X. Hong, Appl. Phys. Lett. **103**(11), 112903 (2013).
[20]Y. Wu, X. Li, A. M. Jonas, and Z. Hu, Phys. Rev. Lett. **115**(26), 267601 (2015).
[21]W. J. Hu, D.-M. Juo, L. You, J. Wang, Y.-C. Chen, Y.-H. Chu, and T. Wu, Sci. Rep. **4**, 4772 (2014).
[22]S.-M. Yoon, S.-W. Jung, S. Yang, S.-H. K. Park, B.-G. Yu, and H. Ishiwara, Curr. Appl. Phys. **11**(3 Supplement), S219 (2011).
[23]Y. H. Zou, L. Han, G. L. Yuan, J. L. Wang, S. Sun, J. L. Sun, X. J. Meng, and J. H. Chu, Ferroelectrics **488**(1), 154 (2015).
[24]M. G. Kim, D. H. Han, K. E. Park, and B.-E. Park, Appl. Phys. Lett. **109**(16), 163502 (2016).
[25]S. Deepa, Deepak, and A. Garg, Phys. Chem. Chem. Phys. **18**(42), 29478 (2016).
[26]G.-G. Lee, E. Tokumitsu, S.-M. Yoon, Y. Fujisaki, J.-W. Yoon, and H. Ishiwara, Appl. Phys. Lett. **99**(1), 012901 (2011).
[27]S.-M. Yoon, S. Yang, and S.-H. K. Park, J. Electrochem. Soc. **158**(9), H892 (2011).
[28]T. N. Ng, B. Russo, B. Krusor, R. Kist, and A. C. Arias, Org. Electron. **12**(12), 2012 (2011).
[29]R. H. Kim, H. J. Kim, I. Bae, S. K. Hwang, D. B. Velusamy, S. M. Cho, K. Takaishi, T. Muto, D. Hashizume, M. Uchiyama, P. André, F. Mathevet, B. Heinrich, T. Aoyama, D.-E. Kim, H. Lee, J.-C. Ribierre, and C. Park, Nat. Commun. **5**, 3583 (2014).
[30]S. K. Hwang, I. Bae, R. H. Kim, and C. Park, Adv. Mater. **24**(44), 5910 (2012).
[31]L. Petti, N. Munzenrieder, G. A. Salvatore, C. Zysset, T. Kinkeldei, L. Buthe, and G. Troster, IEEE Trans. Electron Devices **61**(4), 1085 (2014).
[32]X. Chen, X. Tang, X.-Z. Chen, Y.-L. Chen, X. Guo, H.-X. Ge, and Q.-D. Shen, Appl. Phys. Lett. **106**(4), 042903 (2015).
[33]M. A. Haque and M. T. A. Saif, Proc. Natl. Acad. Sci. U. S. A. **101**(17), 6335 (2004).
[34]S. B. Lang and S. Muensit, Appl. Phys. A **85**(2), 125 (2006).
[35]T. Furukawa, Adv. Colloid Interface Sci. **71**, 183 (1997).
[36]S. Baskaran, N. Ramachandran, X. He, S. Thiruvannamalai, H. J. Lee, H. Heo, Q. Chen, and J. Y. Fu, Phys. Lett. A **375**(20), 2082 (2011).
[37]S. Poddar and S. Ducharme, Appl. Phys. Lett. **103**(20), 202901 (2013).
[38]S. Poddar and S. Ducharme, J. Appl. Phys. **116**(11), 114105 (2014).
[39]E. Fukada, G. M. Sessler, J. E. West, A. Berraissoul, and P. Günther, J. Appl. Phys. **62**(9), 3643 (1987).
[40]Y. Kim, W. Kim, H. Choi, S. Hong, H. Ko, H. Lee, and K. No, Appl. Phys. Lett. **96**(1), 012908 (2010).
[41]H. Lu, C.-W. Bark, D. Esque de los Ojos, J. Alcala, C. B. Eom, G. Catalan, and A. Gruverman, Science **336**(6077), 59 (2012).
[42]R. Cai, V.-A. Antohe, Z. Hu, B. Nysten, L. Piraux, and A. M. Jonas, Adv. Mater. **29**(6), 1604604 (2017).